



HAL
open science

Automatic sensor-based detection and classification of climbing activities

Jérémie Boulanger, Ludovic Seifert, Romain Hérault, Jean-François Coeurjolly

► **To cite this version:**

Jérémie Boulanger, Ludovic Seifert, Romain Hérault, Jean-François Coeurjolly. Automatic sensor-based detection and classification of climbing activities. *IEEE Sensors Journal*, 2016, 16 (3), pp.742-749. 10.1109/JSEN.2015.2481511 . hal-01225056

HAL Id: hal-01225056

<https://hal.science/hal-01225056>

Submitted on 9 Nov 2015

HAL is a multi-disciplinary open access archive for the deposit and dissemination of scientific research documents, whether they are published or not. The documents may come from teaching and research institutions in France or abroad, or from public or private research centers.

L'archive ouverte pluridisciplinaire **HAL**, est destinée au dépôt et à la diffusion de documents scientifiques de niveau recherche, publiés ou non, émanant des établissements d'enseignement et de recherche français ou étrangers, des laboratoires publics ou privés.



Distributed under a Creative Commons Attribution 4.0 International License

Automatic sensor-based detection and classification of climbing activities

J eremie Boulanger, Ludovic Seifert, Romain H erault, Jean-Francois Coeurjolly

Abstract—This article presents a method to automatically detect and classify climbing activities using inertial measurement units (IMUs) attached to the wrists, feet and pelvis of the climber. The IMUs record limb acceleration and angular velocity. Detection requires a learning phase with manual annotation to construct the statistical models used in the cusum algorithm. Full-body activity is then classified based on the detection of each IMU.

I. INTRODUCTION

The sport of rock climbing requires the use of both upper and lower limbs, as climbers reach and grasp holds and use their feet to climb the rock surface. Yet rock climbing encompasses more than continuous upward body movement, because more or less static positions are also crucial for exploring and grasping surface holds [1][2][3], posture regulation [4][5][6][7], arm release and resting [8], and finding routes [9][10].

The time spent in exploration and posture regulation as opposed to ascending, or more broadly the time spent immobile as opposed to in motion, can be analysed by quantifying the durations when the pelvis is and is not in motion [11][8][12][13]. In [11], it was noted that advanced climbers spent 63% of a climb immobile and 37% in actual ascending.

As previously noted, periods of immobility may not represent only inappropriate stops, but rather could reflect active resting [8]. For example, in [14], expert climbers were shown to spend a greater proportion of their climbing time in static states and more of the static time actively resting (i.e. limb shaking), compared with climbers of intermediate skill.

J. Boulanger is working with the University of Rouen, France. email: jeremie.boulanger1@univ-rouen.fr and is funded by the ANR Dynamov.

L. Seifert is working with the University of Rouen, France. email: ludovic.seifert@univ-rouen.fr.

R. H erault is working with the INSA of Rouen, France. email: romain.herault@insa-rouen.fr.

JF. Coeurjolly is working with the Laboratoire Jean Kuntzmann of Grenoble, France. email: jean-francois.coeurjolly@upmf-grenoble.fr

However, a point of difference with [12][13] is that in [14] the variability in limb behaviour was associated with exploration or a more functional use of climbing wall properties. This suggests that during stops climbers may exhibit behaviours that are dedicated to more than managing fatigue.

Ascending requires skills in route finding, which reveals the ability of climbers to interpret the ever-changing structure of the climbing wall design [9][10]. Route finding is a critical climbing skill that can be identified by differentiating exploratory movements and performatory movements [2]. In [2], a distinction between exploratory and performatory movements was made according to whether a potential hold on a climbing wall was touched, irregardless of whether it was used as a support. For example, the authors of [3] reported that skilled climbers tended to touch fewer than three surface holds before grasping the functional one.

Clearly, an excessive duration spent immobile for route finding, hold exploration or posture regulation is likely to compromise climbing fluency and lead to the onset of fatigue. The aim of this article is to propose a method to automatically detect and quantify some of the major climbing activities: immobility, postural regulation, hold exploration, hold change and traction. As stated in [12][13], these activities can only be defined by taking into account the activities of both the limbs and the pelvis.

II. DATA AND PROTOCOL

A. State of the art

Previous studies like those of [11] and [15] focused on rock climbing and analysed the climbers behaviour. This was accomplished by making video recordings of the climb and having experts manually perform the analysis. This method has several drawbacks, as the possibilities for analysis are limited, the results are of relatively low accuracy, and the process itself is long and tedious. Moreover, a full view of the climbing wall might not be available for video recording in outdoor studies without the use of drones or similar devices.

Automatic measures were reported in [16] and [1], with force sensors placed inside the holds on the climbing walls. Despite the high cost of the experimental devices for long routes, this method is not usable outdoors and requires a long set-up for indoor walls that are not yet equipped.

Given the disadvantages of these methods, wireless sensors placed on the climber might be a good solution, offering easy measurement set-up and quick adaptation to the route environment (indoors or outdoors). In [17], for example, the climber carried a single miniature accelerometer that was used to evaluate different performance coefficients. However, this article did not present an analysis of behaviour or a procedure for distinguishing activities and their distribution along the climb. It also did not assess the activities of the different limbs, which is needed to determine the climber state on the climbing wall. This article presents a method using multiple inertial measurement units (IMUs) placed on several body sites, with each IMU containing an accelerometer, a gyroscope and a magnetometer to detect limb and pelvic activities based on their acceleration or angular velocity. This step, presented in Section III, requires learning statistical modelling with a labelled set of climbs, which is accomplished by manual annotation on video recordings of climbing experts. However, these videos are no longer needed once the learning protocol is completed, and Section IV presents a procedure for determining full-body activity by combining the independent detections of limb activity.

B. Protocol

Two male climbers of ability 6a on the French Rating Scale of Difficulty (F-RSD) [18], which corresponds to an intermediate performance level [19], undertook an easy, top-roped route (grade of 5c on F-RSD) composed of 20 hand holds for a 10m height. The route was identifiable by colour and set on an artificial indoor climbing wall by two certified route setters who ensured that it matched an intermediate level of climbing performance. The participants were instructed to self-pace their ascent and to climb fluently and without falling. The ascents were preceded by 3 minutes of route preview, as pre-ascent visual inspection is a key parameter of climbing performance [8]. Procedures were explained to the climbers, who then gave written informed consent to participate¹.

Each climber was considered to be in one the following states at any given time: immobility, postural

¹The protocol was approved by the local University ethics committee and followed the declaration of Helsinki.

regulation, hold exploration, hold change or traction. As stated previously, a single detection of limb activity is required to describe the full-body state.

Accelerations and angular velocities were collected from the four limbs and pelvis using IMUs located on the right and left wrists, right and left feet, and pelvis. The IMUs combined a triaxial accelerometer ($\pm 8G$), a triaxial gyroscope ($1600^\circ/s$) and a triaxial magnetometer (MotionPod, Movea©, Grenoble, France) referenced to magnetic North, sampled at 100Hz. Wireless transmissions to a controller enabled recording with MotionDev-Tool software (Movea©, Grenoble, France). A wearable device is required to measure climbing activities on a 10m-high climbing wall.

C. Recording and preprocessing

The acceleration of each sensor was determined from the recorded signals. These data were used to synchronise the video recording of the climb with the IMU signals in the learning phase of the detection, as well as to detect activity. Therefore, this method had to be used even on unlabelled sets of climbing.

Although the sensors directly record the acceleration in the sensor frame, the recording cannot be used directly as proper acceleration because of the gravity component. The norm of this component is well-known ($9.81m/s^2$), but it cannot be removed from the sensor frame without knowing the orientation of the sensor in the ground reference frame.

Let a_s be the recorded acceleration in the sensor frame. By denoting R the rotation matrix describing the sensor frame in the Earth reference frame (magnetic North, West and vertical up direction), the acceleration a in the Earth reference is then defined as $a = Ra_s$. Once a is obtained, the gravity component can easily be removed (see Figure 1).

To determine R , a complementary filter based algorithm is used [20][21], based on the three sensor information sources (i.e. accelerometer, gyroscope and magnetometer). The gyroscope measures precise angular changes over very short time durations but cannot be used to track the angle changes by integration due to drift. The accelerometer provides absolute, albeit noisy, measurements of acceleration. By combining the two sensor information sources it was possible to reduce the drift of the gyroscope for sensor orientation tracking. When magnetometer information was added, it was possible to compute the sensor orientation respect to the fixed frame of Earth reference.

Figure 2 provides an example of the recorded norm of the processed acceleration signal.

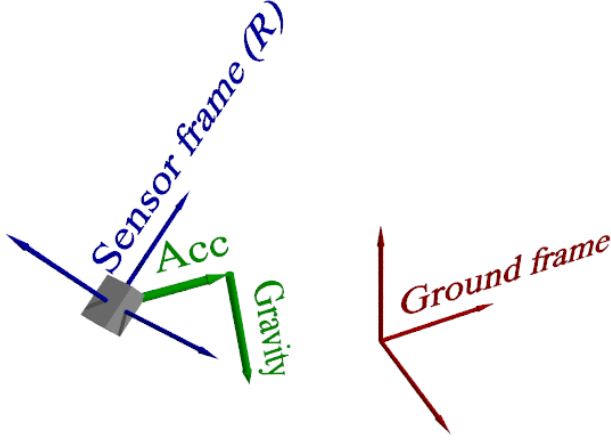


Fig. 1. Example of the frame difference between the ground frame (red), where the gravity is known, *i.e.* can be removed, and the sensor (grey box) frame (blue), where the gravity components are unknown and cannot be removed from the recorded acceleration (sum of the green vectors).

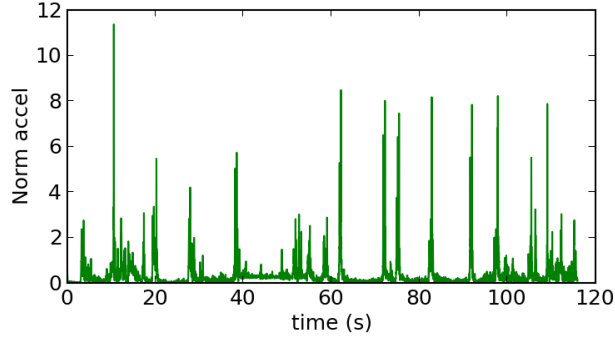


Fig. 2. Example of the evolution in the norm of a recorded acceleration after removing the gravity component. The sensor was attached to the climbers right foot. The acceleration is measured in m/s^2 .

Based on the processed acceleration and the angular velocity, we automatically detected the limb motion using the cusum [22] method.

III. ACTIVITY DETECTION

Activity was detected from each sensor independently. As this method requires a learning phase, this last is also described in detail. Once the learning phase is completed, the paragraph III-A can directly be used.

A. Cusum-based detection

The cusum algorithm is often used to determine a change point in a time series of independent random variables based on statistical models. In this case, we assume that a limb is either immobile (state called H_0) or mobile (in motion) (state H_1) at a given time. It is further

assumed that these states are exhaustive and exclusive, *i.e.* for each sample, the limb is in one of these states and only one. The idea is thus to estimate the state of the limb based on the recorded signals. Let x_t be the considered signal. In our case, it will be the norm of either the acceleration or the angular velocity.

The main idea is to assume that x_t is a random variable sampled from a distribution fixed by the state of the limb. In other words, if the limb is in state H_0 (respectively H_1), then $x_t \sim p(\cdot|H_0)$ (respectively $x_t \sim p(\cdot|H_1)$). If $p(\cdot|H_0)$ and $p(\cdot|H_1)$ are known, a likelihood ratio can be computed for a given t (we directly consider t as a discrete variable, due to the sampling process) to estimate the distribution from which t was sampled

$$l_t^x = \log(p(x_t|H_1)) - \log(p(x_t|H_0)).$$

The sign of l_t^x provides an estimation of the state of the limb at time t : H_1 for positive and H_0 for negative.

It is assumed that the state changing periods are much longer than the sampling time and can therefore form a cumulative sum to increase the detection performance. Let S_t^x be the cumulative sum of the log likelihood ratio

$$S_t^x = \sum_{k \leq t} l_k^x. \quad (1)$$

The propensity of S_t^x to be monotonous indicates the state the limb should be assumed to be in. A change in monotony implies a change in the state. An algorithm looking directly at a change in monotony would be subject to many false detections. Instead, the use of positive thresholds λ_0 and λ_1 helps to reduce false alarms.

For example, given state H_0 at $t = 0$, state H_1 is detected when

$$S_t^x > \min(S_s^x | s < t) + \lambda_1.$$

Similarly, to detect H_0 while being in state H_1 , a change occurs when

$$S_t^x < \max(S_s^x | s < t) - \lambda_0.$$

When a change point is detected, the process starts again by taking the detection time as the new time origin and starting the cumulative sum again from this point.

Although thresholds can be chosen to be equal, we consider a more general framework here by taking different values. These thresholds can influence the false positive detection rate and therefore should be chosen according to a given performance measure or some prior model of detection.

Thresholds as well as the distributions $p(\cdot|H_0)$ and $p(\cdot|H_1)$ are not known in advance in this case, which

is why a learning step is required. A labelled set is used to estimate the distributions and thresholds based on manual annotation, described in the next section.

B. Construction of the labelled set

The climbs were video recorded in their entirety, and experienced climbers manually annotated three different climbs by two different climbers. They indicated for each frame of the video the state of each limb.

Because the camera and sensors were not synchronised, the delay between the frame-based manual annotations and the acceleration had to be estimated. The videos were recorded using a fixed camera facing the wall, with a red light attached to the climbers pelvis. The position of the red light on the image therefore gave the position of the pelvis on the wall, up to some correction. A classical Kalman filter was used to track the red light in the frame, and an adaptive filter was required to counterbalance similar colours in the surrounding environment (in this case, the presence of televisions in the recorded picture). Once the red-light position on the image was obtained, lens distortion had to be corrected, followed by parallax correction. An example of automatic tracking after correction is presented in Figure 3.

Based on the obtained trajectory, an approximate acceleration of the pelvis was determined. Using a maximum correlation measure with the sensor-based lateral and vertical accelerations of the pelvis, the delay between each signal was estimated. Therefore, the manual annotation (based on the video) and the recorded signals (based on the sensors) could be synchronised. An example of correlation is presented in Figure 4.

An example of the synchronised annotation and signal is presented in Figure 6. Based on these annotations, a model was determined for each state. In this example, it appears clearly that the high values of the accelerations match the H_1 hypothesis (mobility). These three annotated climbs, along with the recorded IMU signals, will be used as a labelled set for the learning phase of activity detection.

C. Learning protocol

For now, we consider that $x_t \in \mathbb{R}^+$ is either the norm of the acceleration or the norm of the angular velocity. Using the manual annotations, an example of the histogram of the acceleration norm for each hypothesis H_0 and H_1 is presented in Figure 5.

Instead of considering general distributions for $p(\cdot|H_i)$, $i = 0, 1$, parametric distributions are considered. A χ^2 test is performed for each sensor and each climb

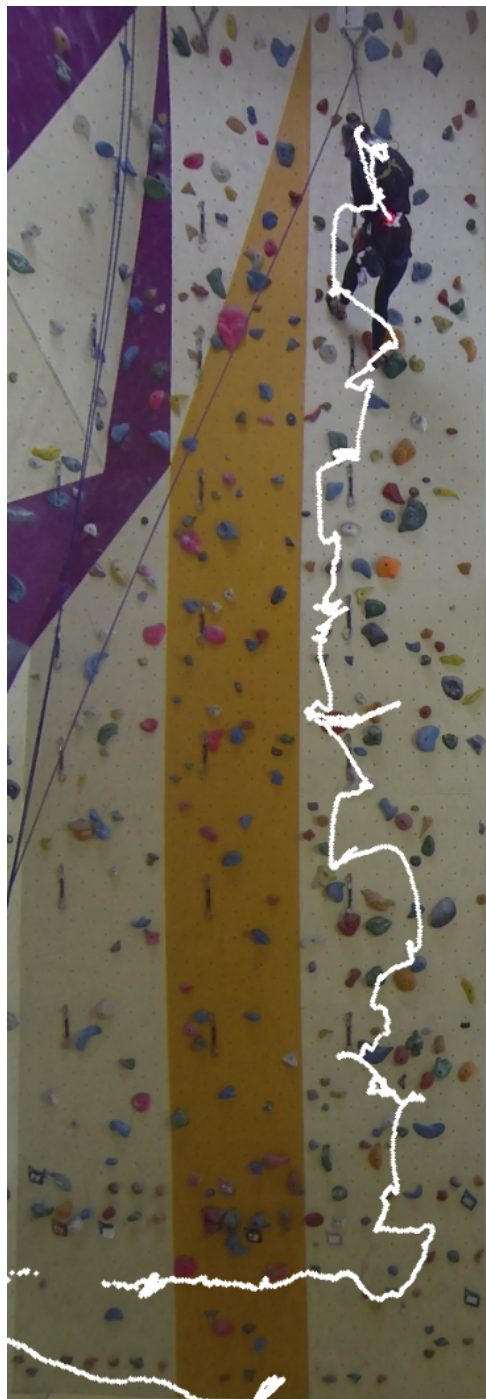


Fig. 3. Example of automatic tracking of the climber based on video footage. The trajectory during the climb is shown in white. The background image is the last image from the video, therefore containing the last tracked position. It is also apparent that the red light can be hidden, for example, due to substantial body rotation so that the light no longer faces the camera. On this image, the lens distortion and the parallax were corrected.

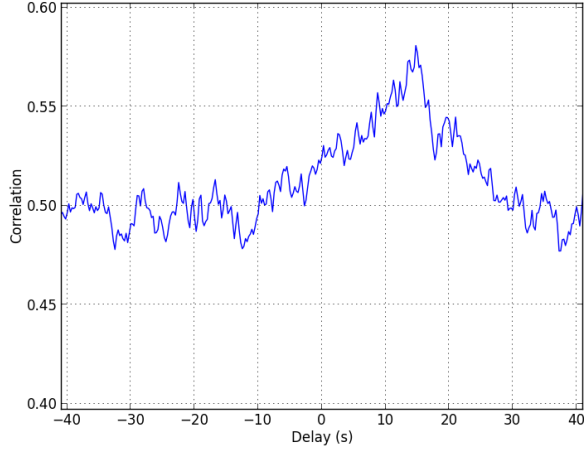


Fig. 4. Example of the correlation between the sensor acceleration and the video tracking-based acceleration. In this case, the delay maximising the correlation is around 14.7s.

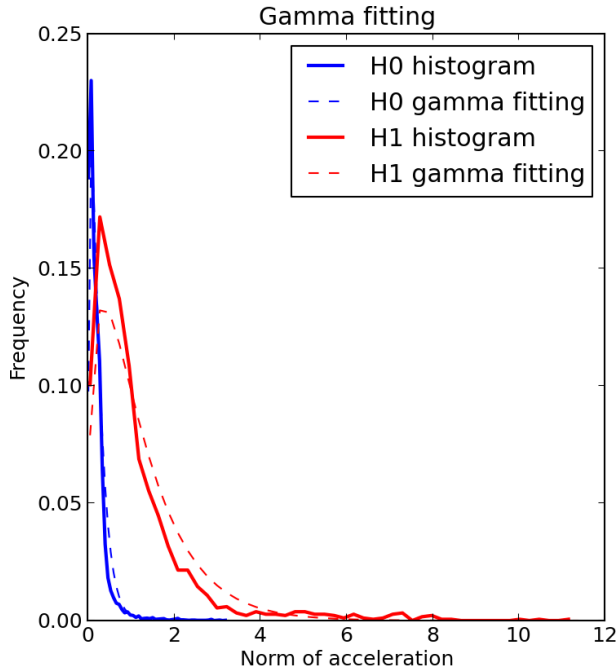


Fig. 5. Comparison between the histogram of the acceleration (solid line) and the fitting Gamma distribution (dotted line). For each state, only the corresponding (based on the annotations from Figure 6) samples are considered. The fitting Gamma distribution is trying to fit the histogram and is obtained via a maximum likelihood estimation.

	Acceleration		Ang. velocity	
	norm	squared	norm	squared
Gamma H_0	1.0	0.68	1.0	0.93
Expone H_0	1.0	0.16	1.0	0.53
Gamma H_1	0.59	0	0.93	0.32
χ^2 H_1	0	0.13	0.28	0.59

Table I
p-values of χ^2 goodness-of-fit tests for the norm and squared norms of the acceleration and angular velocity signals. The Gamma and exponential models are tested for state H_0 , while Gamma and with 3 degrees of freedom models are tested for state H_1 .

and the results are presented in Table I. The values presented in Table I are averages of the p-values for the three annotated climbs. Table I compares the fit between the norm of the acceleration and its squared value to the Gamma distribution, the exponential distribution (which seems to fit the samples in the H_0 hypothesis), and the χ^2 distribution with three degrees of freedom (corresponding, for the squared norm, to a model where each component of the signal is sampled from a Gaussian). It indicates that the Gamma distribution-based model seems a good choice to describe the signals.

To be more specific, we consider the Gamma distributions $p(\cdot|H_i)$ for $i = 0, 1$ for both states given by

$$p(x|H_i) = \frac{1}{\Gamma(k_i)\theta_i^{k_i}} x^{k_i-1} \exp\left(\frac{-x}{\theta_i}\right), \quad (2)$$

where θ_i and k_i are positive real number and $i = 0, 1$ represents the state.

The coefficients θ_i and k_i are determined by maximum likelihood. By considering a second order approximation of the digamma function $\Gamma'(k)/\Gamma(k)$ [23], they are given by

$$\hat{k}_i \approx \frac{3 - s_i + \sqrt{(s_i - 3)^2 + 24s_i}}{12s_i} \quad (3)$$

and

$$\hat{\theta}_i = \mathbb{E}_i[x]/k_i, \quad (4)$$

with

$$s_i = \log(\mathbb{E}_i[x]) - [\mathbb{E}_i[\log(x)]].$$

The term $\mathbb{E}_i[x]$ represents the empirical average of the values of x when the annotation indicates it is in state i . These empirical means are determined by considering the concatenation of the signals from the labeled set.

Clearly, these parameters change with the nature of the signal x_t (norm of the acceleration or norm of the angular velocity).

Based on the signal x_t , using these Gamma distributions with parameters determined via Equations (3) and (4), the cumulated log likelihood ratio S_t^x can be determined. An example is presented, along with the

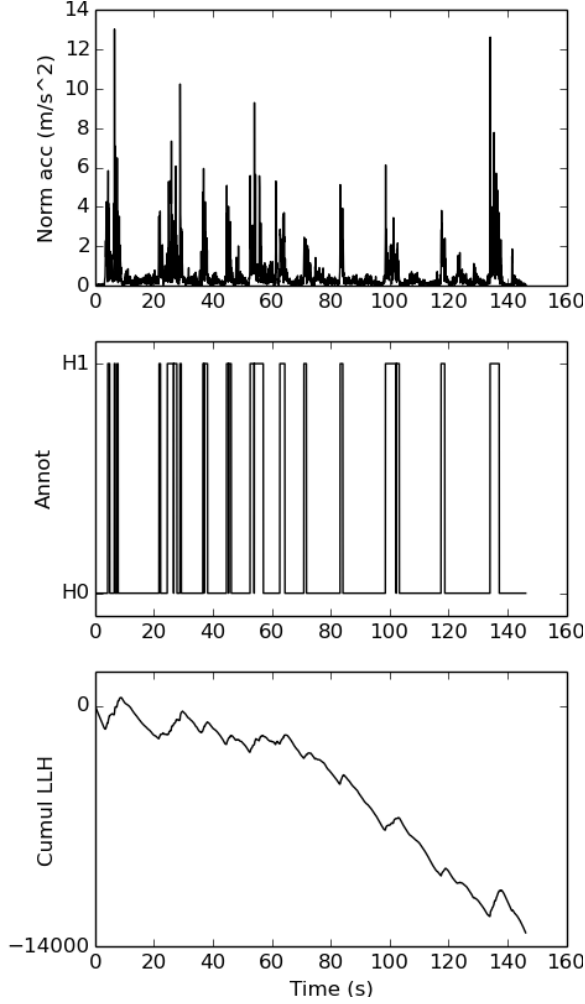


Fig. 6. (Top) Example of the norm of the acceleration for one sensor. (Middle) Manual annotation synchronized with the acceleration signal. (Bottom) Cumulated loglikelihood S_t^{acc} defined in Equation (1) of the acceleration signal using the models constructed from the annotation.

annotations, in Figure 6.

The method presented in Paragraph III-A leads to the determination of a cumulated log likelihood ratio (see Equation (1)), depending on the given signal. Let S_t^{acc} be based on the norm of the acceleration and S_t^{ang} be based on the norm of the angular velocity.

This is due to a lack of proper multivariate Gamma model, preventing the use of both signals directly. Instead, a basic solution is used here where the cumsum algorithm is run on S_t , obtained as a weighted sum of S_t^{acc} and S_t^{ang} :

$$S_t = \alpha S_t^{acc} + (1 - \alpha) S_t^{ang} \quad (5)$$

where $\alpha \in [0, 1]$. For example, if $\alpha = 0$ (respectively

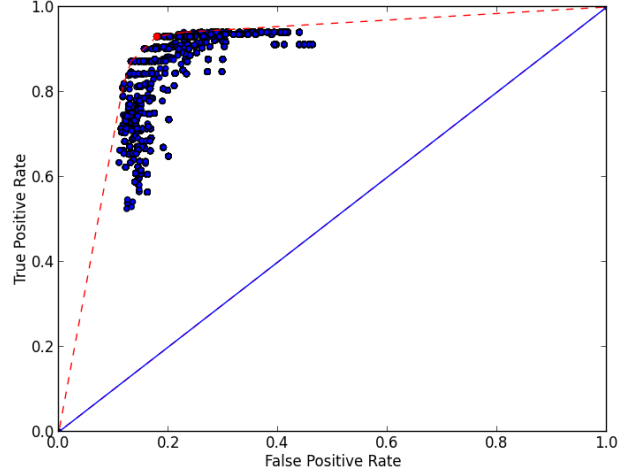


Fig. 7. Example of a ROC figure, representing the true positive rate with respect to the false positive rate. Each dot represents an estimation for a given set of thresholds. The best set of thresholds maximising (6) is the one maximising the distance to the diagonal. In this example, the norm of the angular velocity was the signal used for detection and the sensor was attached to the left foot.

1), then only the angular velocity (respectively acceleration) is considered for detection. A comparison of the performances depending on α is presented in Section III-D. It should be noted that although S_t^{acc} and S_t^{ang} are cumulated log likelihood ratios, S_t is no longer one as the only possible distribution associated with such a likelihood would not be unitary. Therefore, maximising (5) does not correspond to maximising a likelihood. The minimisation of S_t should be regarded as a minimum contrast estimation method.

Running the cusum algorithm with different thresholds λ_i will clearly lead to different estimates. To measure the performance of the detection, the coefficient

$$c = \frac{TP}{P} - \frac{FP}{N} \quad (6)$$

is used, where TP is the number of true positives (detecting H_1 when it is H_1), P (respectively N) the number of elements in H_1 (respectively H_0) in the manual annotation, and FP the number of false positives (detecting H_1 when it is H_0). This coefficient corresponds to the performance measure used in the learning protocol as it represents, in a ROC curve, twice the distance to the diagonal, indicating a random decision (Figure 7). The thresholds are then determined as the ones maximising c .

A comparison of the recorded signal, the annotation and the (optimal) detection is presented in Figure 8. This figure also illustrates the difference between the detection based on other annotations where all the parameters

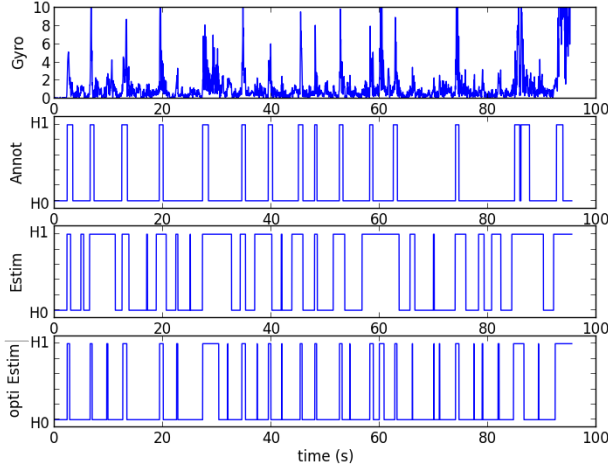


Fig. 8. (Top) Norm of the angular velocity. (Middle top) Manual annotation. (Middle bottom) Detection. (Bottom) Optimal estimation. In this case, the sensor was attached to the right hand. For better readability, the weighted coefficient $\alpha = 0$ was chosen; therefore, only the angular velocity was used in the determination of S_t . It is notable that the optimal estimation still differs from the annotation.

are learnt from a distinct labelled set and the optimal detection based on the signal using the annotation of the signal itself to perform the detection. This optimal detection is not achievable in practice as it requires the annotation of the considered climb.

The next section presents the performance of this detection via a cross-validation method.

D. Performance and limitations

A cross-validation method was used to evaluate the performances of the learning algorithm. The method consists of learning the different parameters (k_i , θ_i , λ_i for $i = 0, 1$), concatenating two out of the three annotated climbs, and applying these parameters on the third one. The annotation for the third climb makes it possible to determine a performance measure via the coefficient from (6). An optimal coefficient c can also be determined by directly learning all the parameters only using the third climb. This gives an idea of the best achievable performance. Then, permutations between the learning and testing climbs are made and the average coefficient c is considered as the final performance of the algorithm. Table II presents the results from the cross-validation for all the sensors for $\alpha = 0, 1$ and the value maximising the score (and therefore, better than the extrema value). It appears that the score is roughly similar for the different values of α . However, the optimal value of α (different for each sensor) will be used from now on. For further applications with

	Acceleration		Ang. velocity		(Accel, Ang vel)	
	score	optimal	score	optimal	score	optimal
L Foot	0.79	0.80	0.80	0.81	0.67	0.82
R Foot	0.74	0.80	0.75	0.83	0.64	0.84
L Hand	0.47	0.62	0.53	0.64	0.48	0.68
R Hand	0.42	0.53	0.43	0.60	0.37	0.59
Pelvis	0.31	0.38	0.34	0.48	0.11	0.49

Table II

Score and optimal score of the cross-validation for $\alpha = 0$ (Ang. velocity), $\alpha = 1$ (Accel) or the optimal α . The score is only slightly increased for the optimal value.x

non-annotated climbs (see Paragraph IV-C), the learning phase is carried out on all three annotated climbs.

The optimal detection did not provide a very high performance measure in all cases. This may have had several causes:

- Missing a movement during manual annotation: Due to the lack of visibility of the concerned limb.
- Delay or different movement period: As the annotation is manual, a delay might occur between a movement and its detection by the person annotating the video.
- Sensor is hit during the climb: For example, this occurs when the climber claps his hands together, creating an acceleration peak of both wrist sensors.
- Defective orientation estimation: As the acceleration signal requires the sensor orientation, a wrong orientation estimation will directly add bias to the acceleration because the gravity component will no longer be aligned with the vertical (according to the sensor).

The next section presents how these binary detections (state H_1 or H_0) from each sensor can be classified to describe a full-body state and how this is used to measure exploration during a climb.

IV. ACTIVITY CLASSIFICATION

A. Full-body activity

Based on state detection of the four limbs and pelvis, we defined four exclusive states matching the different activities of the climber:

- Immobility: All limbs are immobile and the pelvis is immobile.
- Postural Regulation: All limbs are immobile and the pelvis is moving.
- Hold interaction: At least one limb is moving and the pelvis is immobile.
- Traction: At least one limb is moving and the pelvis is moving.

Immobility is the state when the climber is not moving at all. He might be resting due to fatigue or looking at the route to determine its climbing path, while his limbs remain immobile.

Postural regulation is the adjustment of the climbers centre of mass while his limbs stay on the same holds. This might consist of a body rotation to be able to catch a hold that would not be reachable with the previous body configuration.

Hold interaction is the movement of a limb while maintaining the pelvis (and therefore the global position of the climber on the wall) immobile. This is a change in the hold in use before the next traction, a change in the position and orientation of the hand/foot on an hold for better adapted use of the hold, or successive limb movement to determine which hold is most appropriate for the next traction. In the next section, we present a more detailed classification to differentiate actual use of a hold from hold exploration.

Traction is the state when the climber is moving (generally upward) using at least one limb. Although the limb might not be moving as substantially as during a hold change, this state is still easily detected and its definition seems to fit the climbers actual traction phases on the video.

An example of the successive states for a climb is presented in the last panel of Figure 10.

B. Limb state

It quickly appears that the state of hold interaction covers a wide spectrum of activities. It is not directly possible to determine whether the climber is actually using a hold or moving a limb towards different holds to check whether they are reachable and, if so, how to use them (in this case, the limb can remain on the same hold but change its orientation). Consequently, new states for each limb are considered as sub-states of the Hold interaction defined in Section IV-A. These sub-states are the following:

- Immobility: When a limb is detected as being immobile.
- Use: When a limb is moving during traction.
- Change: The last movement before traction, or the final change in hold (or change in limb orientation on the same hold) before being used.
- Exploration: All movements except the last one before traction. An example is the case when the climber is trying several holds before choosing the one he will be using for traction.

A summary of the different states is presented in Figure 9 and an example of the full state analysis of a climb is

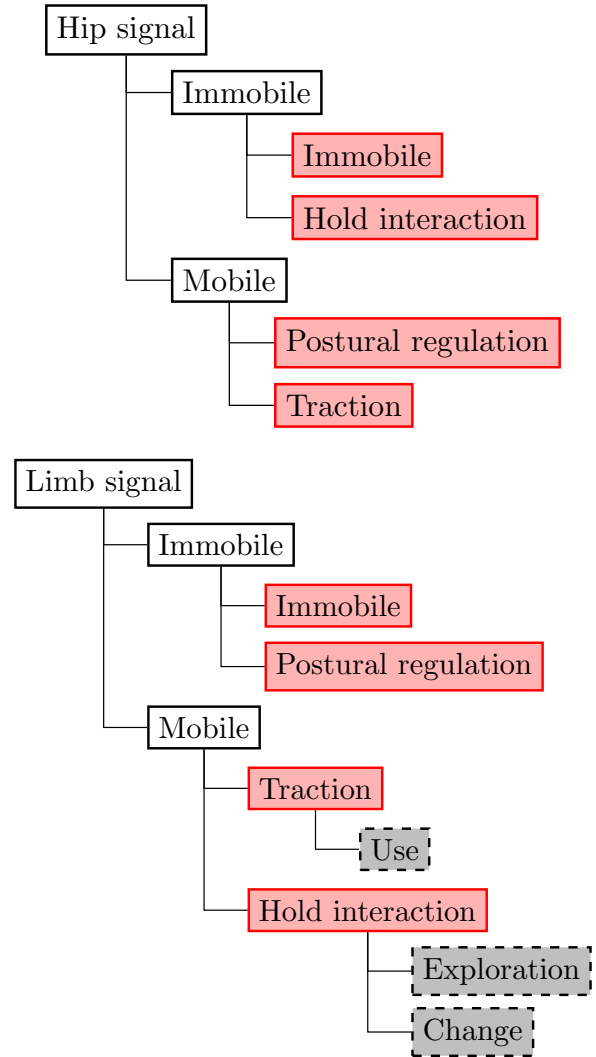


Fig. 9. Decision tree from the signals. White rectangles are decisions from single sensors and red rectangles are multiple sensor decisions. Each decision depends on the decisions from other sensors. The last layer for the limb detection tree depends on the next traction detection.

presented in Figure 10.

C. Example of application

This section presents a simple example of application based on the previous algorithm: measuring the ratio between exploratory and performatory movements.

As previously noted, this ratio can be used to differentiate skilled and unskilled climbers [3], which makes automatic detection of the ratio very useful. Based on the present algorithm, *Exploration* and *Change* encompass all the exploratory movements for each limb, whereas

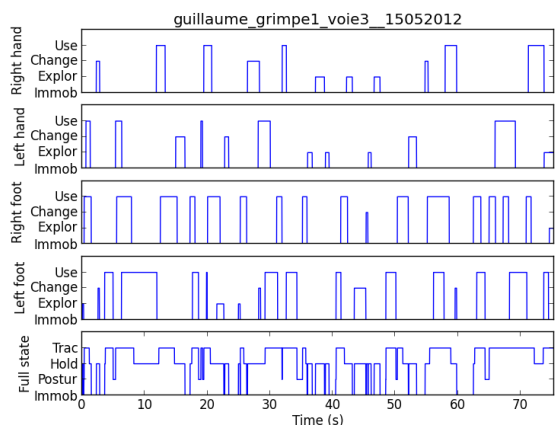


Fig. 10. Example of classification from a non annotated climb. From top to bottom: full state evolution for each limb: right hand, left hand, right foot, left foot and full body state evolution during the climb.

Use reflects only the performatory movements. The results based on a total of 94 climbs by three experts and three beginners on a 10m-high climbing route are presented in Figure 11. A distinction between experts and beginners clearly emerges based on the ratio between these quantities.

Like previously stated, it has been shown [3] that this ratio can be used to differentiate skilled and unskilled climbers. There is therefore an interest in automatically detecting this ratio. Based on the present algorithm, the number of exploratory movements will gather, for each limb, the number of *Exploration* and *Change* while the number of performatory movement only counts the *Use* activity periods. Results based on a total of 94 climbs realized by 3 experts and 3 beginners on a 10 meters high climbing route are presented in Figure 11. A distinction between experts and beginners clearly appears considering the ratio between these quantities

It should be noted that some of the values from this figure seem rather high for a 10m-high climbing route. This is partly due to the computation of the sensor orientation, which is still somewhat inexact. If the orientation is not properly determined, the computed acceleration contains residuals from the gravity component, inducing a *mobile* phase detection further on and misleading the counting process. One possibility to eliminate this issue might be to only consider the angular velocity value, as the performances do not differ significantly between angular velocity and acceleration use. Another factor might be individual differences between the climbers from the labelled set used for the learning protocol and the climbers used in this application. To prevent this

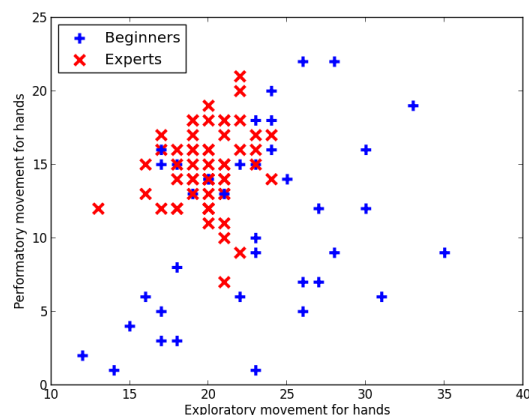


Fig. 11. Comparison between the number of holds touched by the hands (exploratory movement) and the number of holds used (performatory movement) during a climb. Results for the feet are quite similar. A classification clearly appears based on the ratio between these quantities.

individual dependent measure, the learning phase can be accomplished using a dedicated climber recording and the learnt parameters only for this specific climber.

V. CONCLUSION

This article presents a method for the automatic detection and classification of climbers activities based on multiple IMUs. From a learning phase requiring manual annotations, a statistical model is built for the norms of acceleration and angular velocity. This model is used in a cusum algorithm to detect a binary movement state for each limb with an attached sensor. The concatenation of the states of each sensor is used to determine and classify full-body activity. A more detailed classification is then used to measure exploration during the climb.

Determining exploratory activity during climbing is useful as it provides a measure of skill and learning performances. Future works will focus on the use of this method in a learning protocol for indoor climbing, measuring the occurrence and distribution of exploration and immobility in the participants. Another study on immobility is planned to determine which body configurations are mainly used during learning and how these configurations evolve from climb to climb during a learning protocol

REFERENCES

- [1] F. Fuss and G. Niegl, "Instrumented climbing holds and performance analysis in sport climbing," *Sports Technology*, vol. 1, pp. 301–313, 2008.

- [2] J. R. Pijpers, R. D. Oudejans, F. Bakker, and P. J. Beek, "The role of anxiety in perceiving and realizing affordances," *Ecological Psychology*, vol. 18, pp. 131–161, 2006.
- [3] F. Sibella, I. Frosio, F. Schena, and N. A. Borghese, "3d analysis of the body center of mass in rock climbing," *Human Movement Science*, vol. 26, 2007.
- [4] C. Bourdin, N. Teasdale, and V. Nougier, "High postural constraints affect the organization of reaching and grasping movements," *Experimental Brain Research*, vol. 122, pp. 253–262, 1998.
- [5] C. Bourdin, N. Teasdale, V. Nougier, C. Bard, and M. Fleury, "Postural constraints modify the organization of grasping movements," *Human Movement Science*, vol. 18, pp. 87–102, 1999.
- [6] M. Testa, L. Martin, and B. Debû, "Effects of the type of holds and movement amplitude on postural control associated with a climbing task," *Gait and Posture*, vol. 9, pp. 57–64, 1999.
- [7] —, "3d analysis of posturo-kinetic coordination associated with a climbing task in children and teenagers," *Neuroscience Letters*, vol. 336, 2003.
- [8] X. Sanchez, P. Lambert, G. Jones, and D. J. Llewellyn, "Efficacy of pre-ascent climbing route visual inspection in indoor sport climbing," *Scandinavian Journal of Medicine and Science in Sports*, vol. 22, pp. 67–72, 2012.
- [9] P. Cordier, M. Mendès-France, P. Bolon, and J. Pailhous, "Entropy, degrees of freedom, and free climbing: a thermodynamic study of a complex behavior based on trajectory analysis," *International Journal of Sport Psychology*, vol. 24, pp. 370–378, 1993.
- [10] —, "Entropy as a global variable of the learning process," *Human Movement Science*, vol. 13, pp. 745–763, 1994.
- [11] V. Billat, P. Palleja, T. Charlaix, P. Rizzardo, and N. Janel, "Energy specificity of rock climbing and aerobic capacity in competitive sport rock climbers," *The Journal of Sports Medicine and Physical Fitness*, vol. 35, pp. 20–24, 1995.
- [12] L. Seifert, D. Orth, R. Héroult, and K. Davids, "Affordances and grasping patterns variability during rock climbing," *Studies in Perception and Action XII: Seventeenth International Conference on Perception and Action*, 2013.
- [13] L. Seifert, L. Wattebled, R. Héroult, G. Poizat, D. Adé, N. Gal-Petitfaux, and K. Davids, "Neurobiological degeneracy and affordance perception support functional intra-individual variability of inter-limb coordination during ice climbing," *PLoS One*, vol. 9, 2014.
- [14] S. Fryer, T. Dickson, N. Draper, M. Eltom, L. Stoner, and G. Blackwell, "The effect of technique and ability on the vo2heart rate relationship in rock climbing," *Sports Technology*, vol. 5, pp. 143–150, 2012.
- [15] D.J. White and P.D. Olsen, "A time motion analysis of bouldering style competitive rock climbing," *The Journal of Strength and Conditioning Research*, vol. 24, p. 1356, 2010.
- [16] F. Quaine, L. Martin, and J.P. Blanchi, "The effect of body position and number of supports on wall reaction forces in rock climbing," *Journal of Applied Biomechanics*, vol. 13, pp. 14–23, 1997.
- [17] J. Pansiot, R. King, D. McIlwraith, B. Lo, and G. Yang, "Climbsn: Climber performance monitoring with bsn," *International Workshop on Wearable and Implantable Body Sensor Networks*, vol. 5, pp. 33–36, 2008.
- [18] D. Delignières, J. Famose, C. Thépeaut-Mathieu, and P. Fleurance, "A psychophysical study of difficulty rating in rock climbing," *International Journal of Sport Psychology*, vol. 24, pp. 404–416, 1993.
- [19] N. Draper, T. Dickson, G. Blackwell, S. Fryer, S. Priestley, D. Winter, and G. Ellis, "Self-reported ability assessment in rock climbing," *Journal of Sports Sciences*, vol. 29, pp. 851–859, 2011.
- [20] S. Madgwick, *An efficient orientation filter for inertial and inertial/magnetic sensor arrays*, 2010.
- [21] S. O. H. Madgwick, A. J. L. Harrison, and A. Vaidyanathan, "Estimation of imu and marg orientation using a gradient descent algorithm," *International Conference on Rehabilitation Robotics*, 2011.
- [22] P. Granjon, *The CUSUM algorithm, a small review*, 2012.
- [23] T.P. Minka, *Estimating a Gamma distribution*, 2002.